Voxel-based analysis of high- and standard b-value diffusion weighted imaging, and voxel based morphometry, in Alzheimer disease

E. De Vita[1,2], B. H. Ridha[3], N. C. Fox[3], J. S. Thornton[1,2], and H. R. Jager[1,2]

[1]Lysholm Department of Neuroradiology, National Hospital for Neurology and Neurosurgery, London, United Kingdom, [2]Academic Neuroradiological Unit, Department of Brain Repair and Rehabilitation, UCL Institute of Neurology, London, United Kingdom, [3]Dementia Research Centre, Department of Neurodegenerative Diseases, UCL Institute of Neurology, London, United Kingdom

Introduction. Diffusion weighted imaging (DWI) has been used widely to study Alzheimer's disease (AD), traditionally employing a region of interest (ROI) analysis approach [1]. More recently diffusion tensor imaging (DTI) metrics have been analysed on [2] or along specific white matter tracts [3] or over all principal white matter (WM) structures using TBSS [4]. In most of these studies, standard diffusion-weighting, typically b~1000s/mm^2 (b1k) was employed. However, in certain pathologies, higher diffusion-weightings (e.g. b~3000s/mm^2; b3k), which is more sensitive to tissue-water components exhibiting restricted diffusion, has shown an increased pathological sensitivity [5-7]. One AD DTI study used an ROI analysis and reported higher sensitivity to WM degeneration for higher b-values, up to 4000s/mm^2 [8]. Another study used a whole-brain histogram analysis to suggest that high-b q-space (acquiring DWI data with b up to 14000s/mm^2) is more sensitive than DTI to AD and vascular dementia pathology [9]. However, both studies lacked a detailed regional assessment of the findings across the whole brain. We used voxel based analysis (VBA) to investigate the relative pathological sensitivity of b1k and b3k acquisitions over the whole brain (DWI-VBA); and compare these results with an assessment of regional brain atrophy (voxel based morphometry, VBM [10]) in the same AD cohort.

Methods. ***Patients and MRI.*** 11 AD patients (age 69/56-81 yrs (median/range); 6 males; MMSE 16.7±6.2) and 12 healthy controls (Ctr; age 62/54-77 yrs; 6 males; MMSE 26.8±6.4) were examined at 1.5T (GE Signa LX). Acquisitions: for structural imaging a 3D-IR-SPGR sequence (TR/TE 5/35ms, flip angle 35º, resolution 0.9x1.9x1.5mm^3); for DWI, a single-shot EPI (TR 10s, resolution 2.7x2x5 mm^3, b=0 plus 3 orthogonal directions for b1k (TE 101ms, 1 avg) or b3k (TE 136ms, 3 avg).

Data Processing and Analysis. Apparent diffusion coefficient (ADC or mean diffusivity) was calculated using b=0 and trace-weighted b>0 data according to $S_{1k,3k}=S_{b=0}*exp(-\ b_{1k,3k}*ADC_{1k,3k})$. VBA and VBM were performed with SPM8 [11] using 'unified segmentation' [12], and DARTEL [13] (default parameters) to generate cohort-specific grey and white matter (GM, WM) templates at 1.5mm isotropic resolution. Individual subject GM and WM segments were warped to these templates and smoothed (6mm Gaussian kernel). For statistical analysis masks were generated with the 'optimal threshold' method [14] on the resulting average WM and GM data separately. For DWI-VBA, affine transformations were estimated between the b=0 ($b0_{1k}$, $b0_{3k}$) images and the corresponding T1-volume [15]. The ADC_{1k}, ADC_{3k} images where then warped to the cohort T1-template generated for VBM and smoothed (6mm); the mask comprised the sum of GM and WM masks from VBM. Age and total intracranial volume were used as covariates for both VBM and DWI-VBA. As small vessel disease (assessed by a neuroradiologist with 15 years experience and defined as focal or confluent T2 hyper-intensities in the cerebral and infra-tentorial WM) was present in several subjects (4 per group) this was used as additional covariate to prevent ensuing bias of results by this factor. None of the covariates was significantly different between groups. ADC_{1k}-ADC_{3k} images (Sub_{1k-3k}) were also analysed. T-contrasts for Ctr>AD and Ctr<AD were evaluated. To correct for multiple comparisons voxel-wise false discovery rate (FDR) was used. Additionally, for the b1k *vs* b3k comparison an F-contrast defined a sub-mask where ADC_{1k}(AD)> ADC_{1k}(Ctr) or ADC_{3k}(AD)> ADC_{3k}(Ctr), with an F-threshold of 10.25 (FDR corrected p<0.001). T_{b1k} and t_{b3k} scores, ADC values and the %SD of the residual mean square (ResMS) images after the SPM model fit (calculated as $100*2*\sqrt{(ResMS)/(ADC_{AD}+ADC_{Ctr})}$) were then analysed within this sub-mask.

Results. T-maps for VBM (combined display of GM and WM), (Ctr>AD) and DWI-VBA (AD>Ctr) for b1k, b3k VBA are shown for FDR p<0.01 (t-thresholds: 3.68 (GM), 3.40 (WM), 3.19 (b1k), 3.20 (3k) in figures 1a-c, overlaid on a smoothed average T1 image or ADC1k map. For the opposite contrasts, no supra-threshold voxels were present even at FDR corrected p<0.05. The number of supra-threshold voxels for AD>Ctr was ~95k for b1k and ~92k for b3k with an overlap of ~76k voxels; the mean t scores were: $<t_{b1k}>$= 4.28±0.93 vs $<t_{b3k}>$= 4.39±1.02. The table shows the comparison of b1k and b3k over the common F-mask. Cumulative distribution analysis (fractions of voxels within mask below any given p-value) showed that for b3k, there is slightly greater fraction of voxels than b1k only below an uncorrected p=0.0008 (or t>3.5). Significant changes in Sub_{1k-3k} showed similar regional distribution (but smaller extension, ~47k voxels) as ADC1k and ADC3k, with $<t_{b1k-b3k}>$= 4.38±0.79.

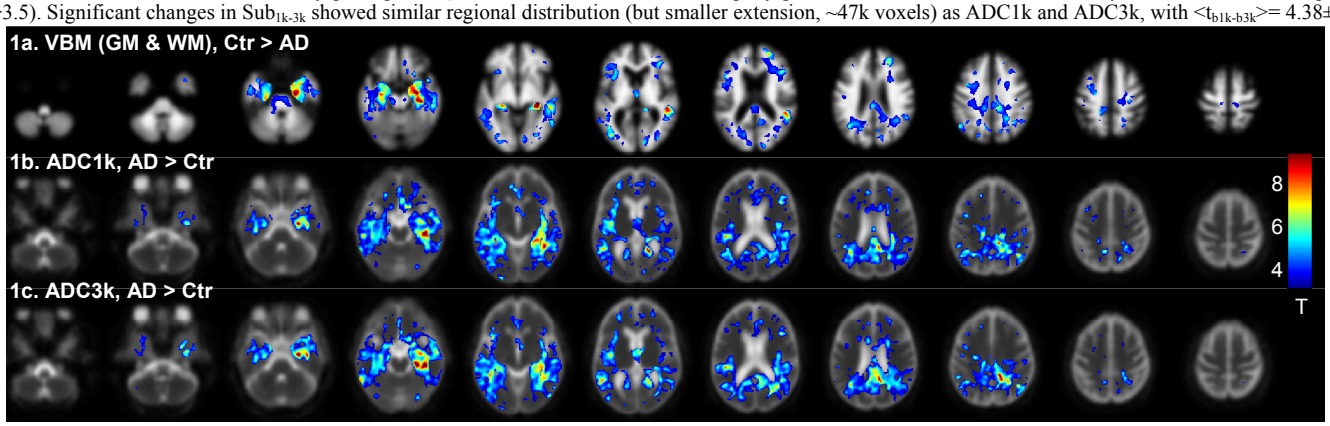

Discussion. In agreement with published literature [16], our voxel based analyses demonstrate widespread pathological changes associated with AD, not limited to medial temporal lobe and involving: temporal WM, splenium of the corpus callosum, parahippocampal WM, posterior portions of the cingulate gyrus and precuneus. There was relative sparing of the frontal lobes, motor cortices, cortico-spinal tracts, coronae radiatae and internal capsules. Overall, with our acquisition parameters, ADC changes appear much more widespread than volumetric (atrophy) changes (i.e. for the same statistical thresholds, many more areas demonstrate significant changes between AD and Ctr groups). With a 3-fold increase in the number of averages for the high-b acquisition, the ADC1k and ADC3k analyses appeared to demonstrate a comparable sensitivity to ADC increase for AD subjects vs controls. ADC1k changes involve slightly more voxels than ADC3k changes. This happens despite the ADC1k data being slightly noisier (see %SD of ResMS), and is due to the fact that the % difference between groups is slightly higher for ADC1k than ADC3k. Indeed, analysis of the difference ADC1k-ADC3k shows a similar distribution of significantly different areas to ADC1k or ADC3k (though over a reduced volume) where Sub_{1k-3k}(AD)>Sub_{1k-3k}(Ctr). This study confirms the value of a combined assessment of volumetric changes and parenchymal tissue diffusion properties. The incomplete overlap of the DWI-VBA and VBM statistical maps underlines the need for integrated operator independent whole-brain approaches [5].

F-mask means	ADC1k	ADC3k	units
Ctr	1055 (267)	741 (138)	10^{-6} mm^2/s
AD	1283 (362)	849 (167)	10^{-6} mm^2/s
AD-Ctr	222 (122)	109 (50)	10^{-6} mm^2/s
% (AD-Ctr)/Ctr	20.4 (8.8)	14.6 (6.4)	%
%SD of ResMS	5.0 (1.8)	3.7 (1.4)	%
T	4.2 (1.0)	4.2 (1.2)	-
P	.004 (.005)	.005 (.060)	-

Conclusions. Although only mean diffusivity was available in this work, the high-b protocol displayed sensitivity to AD pathology comparable to the conventional b1k approach. In contrast with previous studies [9], our analysis suggests there may be no advantage in using high-b DWI, especially given the longer acquisition time needed for comparable SNR.

References. *[1] Sexton CE, Neurobiol Aging, 2010, PMID 20619504 [2] Mielke MM, Neuroimage **46**:47, 2009 [3] Kiuchi K, Brain Research **1287**:184, 2009 [4] Acosta-Cabronero J, Brain 133:529 2010 [5] Hyare H, AJNR **31**:521, 2010 [6] Kim HJ, AJNR **26**:208, 2005 [7] Seo HS, AJNR **29**:458, 2008 [8] Yoshiura T, NeuroImage 20:413, 2003 [9] Mayzel-Oreg O, J Neurol Sci **257**:105, 2007 [10] Ashburner J, Neuroimage **11**:805, 2000 [11] www.fil.ion.ucl.ac.uk/spm/software/spm8 [12] Ashburner J, Neuroimage **26**:839, 2005 [13] Ashburner J, Neuroimage **38**:95, 2007 [14] Ridgway G, Neuroimage **44**:99, 2009 [15] Ourselin S, Image and Vision Computing **19**:25 2001 [16] Braak H, Acta Neuropathologica **82**:239, 1991.*